

GAMMA SAR Systems

Introduction

The GAMMA Synthetic Aperture Radar (SAR) systems are compact and lightweight frequency-modulated continuous-wave (FMCW) imaging radars with four independent receiver channels that can be operated in either single-channel transmission mode or in dual-channel alternating transmission mode. The GAMMA SAR Systems are suitable for high-resolution SAR imaging, single-pass and repeat-pass SAR interferometry, SAR tomography, and polarimetry from automobiles, UAVs (see Figure 1), or piloted aircraft. The versatile SAR systems can be used for a wide range of applications including measurement of ground motion and change detection in repeat-pass interferometric mode, retrieval of surface topography and 3-D vegetation structure, retrieval of snow properties, land use mapping, etc.

This short document describes the SAR system characteristics, sensor platforms/mounts, positioning systems, and the available SAR image processing software. It also contains examples of UAV- and car-based repeat-pass differential interferometry using these instruments.





Figure 1: Gamma L-Band SAR with carbon frame, patch antennas, and integrated GNSS/INS navigation system mounted on a Freefly Alta X quadcopter UAV (left) and a Gamma S-Band SAR mounted on a car roof rack (right) for repeat-pass interferometric SAR acquisitions in single-, dual-, or quad-polarimetric acquisition mode.

SAR sensor characteristics, platforms, and GNSS/INS positioning system

L-band and S-band versions of the GAMMA SAR systems are available with the following key characteristics:

- Gamma L-band SAR (GLSAR), frequencies: 1.2 1.4 GHz, range resolution: 0.75 m
- Gamma S-band SAR (GSSAR), frequencies: 3.0 3.4 GHz, range resolution: 0.38 m
- Azimuth resolution (full synthetic aperture): < 0.2 0.5 m depending on antenna size
- Mass:
 - o radar electronics assembly (REA): 4.2 kg (aluminum box)
 - o total mass of UAV-ready payload: < 6.5 kg (REA + carbon frame with 2 radar antennas, 2 GNSS antennas, and cables)
- Dimensions
 - o radar electronics assembly (REA): 100 x 254 x 254 mm

More details on the SAR system specifications are given in Table 1, p. 12.



Since 2019, GAMMA SAR systems have been used for repeat-pass interferometric measurements on the following **airborne** and **terrestrial** platforms:

- UAVs:
 - o Quad-/Octocopter UAVs: Freefly Alta X¹ and Harris Hx8²
 - o Helicopter UAVs by SUNGWOO Eng.³ and Aeroscout GmbH⁴,
- Terrestrial platforms:
 - o car driving on a road and rail-based measurements,
- piloted aircraft: ongoing integration

A lightweight carbon-fiber frame is available to support the entire SAR system (see Figure 2) including the radar electronics assembly (aluminum enclosure), the radar transmitting (TX) and receiving (RX) antennas, and the navigation system. The navigation system is a Honeywell HGuide n500 GNSS/INS, that consist of a dual-GNSS receiver with antennas (GNSS-1 and GNSS-2) and an inertial measurement unit (IMU), that is built into the radar electronics enclosure. Using this carbon frame, the entire SAR system can be attached to a UAV at a single mounting point or it can be attached to a roof-rack of a car as shown in Figure 1 using a provided adapter. In the UAV configuration shown, the SAR system can acquire fully-polarimetric SAR images and perform repeat-pass interferometric and tomographic measurements.



Figure 2: Left: Gamma L-Band SAR system (without antenna, Ethernet, and power cables) in a carbon frame structure ready for attachment to a UAV or to be mounted on an automobile roof rack. Right: 3-D CAD visualization of the Gamma L-Band SAR with labels and coordinate system definitions.

Example Applications

The GAMMA SAR Systems are compact and can be mounted on various platforms including, UAVs, automobiles, ships, and piloted aircraft with various possible antenna configurations for interferometric and polarimetric applications. These applications include repeat-pass differential interferometry to measure line of sight (LOS) deformation, quad-pol complex backscatter measurements, combined single-track polarimetric interferometry, and SAR tomography. Using two repeat-pass SAR images – or a longer time-series of repeat-pass SAR measurements – surface displacements along the radar line-of-sight (LOS) can be measured. Demonstration cases shown here include mobile mapping of surface displacements (landslide monitoring, glacier flow velocity) by means of car-borne SAR interferometry and a demonstration of UAV-borne repeat-pass interferometric measurements over urban areas and

¹ https://freeflysystems.com/alta-x

² https://harrisaerial.com/carrier-drones/carrier-hx8

³ http://www.swerc.com

⁴ http://www.aeroscout.ch (using a previous version of the Gamma L-Band SAR)



slopes of a mountain valley. By flying multiple repeated parallel tracks with adequate spatial separation, a tomographic stack of SAR data can be obtained and focused to retrieve 3-D structure information of semi-transparent media.

Radar instrument

Table 1 provides a short summary of the GAMMA L-band and S-band FMCW SAR systems specifications configured for the airborne/car-borne acquisition mode. These radars both have four low-noise receiver channels that can be operated simultaneously. A custom FPGA digitizer simultaneously records all four channels and streams radar raw data to SSD memory at up to 60 MB/s. The radar instrument is controlled by a Linux-based (Ubuntu) computer that handles radar configuration, timing, recording navigation and radar data, and monitoring system status. The radar control software and raw data analysis are written in Python3 and are well documented. The radar transmitter max. output is 13W at L-Band and 8W for the S-Band. The transmitter output can be routed to one of two output ports or alternately switched in sync with the radar pulses. The alternating mode is useful for acquiring data that are fully-polarimetric (quad-pol) or have multiple across-track or along-track interferometric baselines.

Total power consumption is typically 100W when acquiring data and ~50W when the radar is quiescent. About 10W of the power consumptions is from the GNSS/INS system.

Accurate positioning with an GNSS/INS system

SAR imaging and interferometric processing of Gamma L-/S-Band SAR data acquired from mobile platforms, UAVs, or piloted aircraft requires centimeter-level (or better) relative positioning accuracy within the SAR sensor trajectory. Hence, the built-in GNSS/INS navigation system is an essential element of the Gamma SAR Systems, ensuring that high-quality SAR images and interferometric data products can be generated. In addition to the built-in Honeywell HGuide n500 GNSS/INS system, an ad-hoc GNSS reference station close to the planned SAR sensor trajectory is typically used to enable GNSS carrier-phase-based post-processed kinematic (PPK) positioning at the highest level of precision and accuracy. Alternatively, a nearby permanent GNSS station or a virtual reference station (VRS) based on a network of permanent GNSS stations can also be used in cases where no ad-hoc GNSS receiver can be set up. The navigation data processing, which requires dedicated software, includes GNSS positioning obtained in PPK mode and GNSS/INS data fusion.

In our SAR campaigns, we have successfully used the GNSS/INS system Honeywell HGuide n580 or the built-in version n500 with Septentrio multi-band GNSS receivers (Altus NR3, AsteRx SB3 ProBase) as ad-hoc GNSS reference stations and Novatel's Waypoint Inertial Explorer Software to process the navigation data with the required positioning accuracy.

It is certainly possible to use other GNSS/INS systems and navigation processing software, but we have not tested these. We can, however, offer guidance with defining an adequate GNSS/INS setup and the required format of the processed GNSS/INS positioning and attitude data to interface it with the TDBP SAR processor. Note, that using other GNSS/INS systems requires either the manufacturer's own navigation processing software or equivalent software such as e.g. Novatel's Waypoint Inertial Explorer.



SAR Image Processing

As a third important element of an end-to-end SAR system on an agile platform, a CUDA/ANSI C [1] implementation of a time-domain back-projection (TDBP) algorithm [2,3] adapted to FMCW systems [1,4,5], is used to focus the airborne or car-borne SAR images directly to map coordinates. The CUDA-GPU-based TDBP processing software is available in combination with the GEO module of the GAMMA software (https://gamma-rs.ch/gamma-software). The following computer hardware and operating system (OS) configurations are supported by the TDBP focusing software: an Ubuntu Linux computer equipped with a recent NVIDIA GPU (global GPU memory: > 10 GB). Specific hardware/OS configurations we have used include Ubuntu Linux 20.04/22.04/24.04. Workstation or high-performance computing versions of NVIDIA GPUs are recommended. An up-to-date NVIDIA GPU (e.g. RTX3000 series or newer) running on a laptop can also be used with the TDBP package.

The TDBP processing approach accurately handles deviations from linear flight trajectories, and in general, non-linear sensor trajectories, given that the sensor trajectory and the topography of the illuminated area are well-known. In this way, focused single-look complex SAR images can be obtained directly in map coordinates. In these geocoded complex SAR images, the topographic phase component is already removed permitting direct computation of differential interferograms. Since the TDBP SAR processing software is executed on the command line, it can also be run on cloud-based instances of Ubuntu Linux machines equipped with an NVIDIA GPU, as e.g. offered by Amazon Web Services (AWS)⁵.

Further processing of focused SAR images is supported by other modules of the GAMMA software, including interferometric processing (ISP/DIFF modules), polarimetric decompositions and filtering (LAT module), interferometric time-series analysis (IPTA module), etc. (https://gamma-rs.ch/gamma-software). The Gamma Software natively supports post-processing of the geocoded SLC images produced by the TDBP processing package. Calculation of interferograms and coherence maps, phase unwrapping, filtering, and time-series analysis are all supported.

Development

Initially, through an R&D project in collaboration with ETH Zurich, supported by the Swiss Innovation Agency Innosuisse, we have performed several car-borne SAR test campaigns to establish, test and integrate the L-band SAR and GNSS/INS instrumentation and to validate the TDBP SAR image focusing and the InSAR processing approach. These R&D activities have been continued in-house at Gamma Remote Sensing to establish and demonstrate further applications and use cases.

⁵ See e.g.: https://docs.aws.amazon.com/AWSEC2/latest/UserGuide/configure-gpu-instances.html



Multi-copter UAV-borne L-band repeat-pass InSAR

UAVs are agile airborne platforms that allow flexible planning and realization of sensor trajectories that are tailored to a specific application. Quadcopter UAV SAR imaging and repeat-pass interferometry with the Gamma L-Band SAR system as shown in Figure 1 was first demonstrated in Pennsauken, NJ, USA, in May 2024. In Figure 3, a SAR image and interferometric phase and coherence maps of repeat-pass DInSAR data acquisitions with a short time interval of a few minutes are shown. For the TDBP SAR focusing, the highly accurate post-processed sensor trajectories and a digital terrain model were used. The high coherence and the smooth phase map indicate the high quality of the SAR imaging and interferometric processing. Only in the near range, residual non-zero spatial baselines in combination with the building/trees, not included in the terrain model, lead to substantial residual non-zero (topographic) interferometric phase.

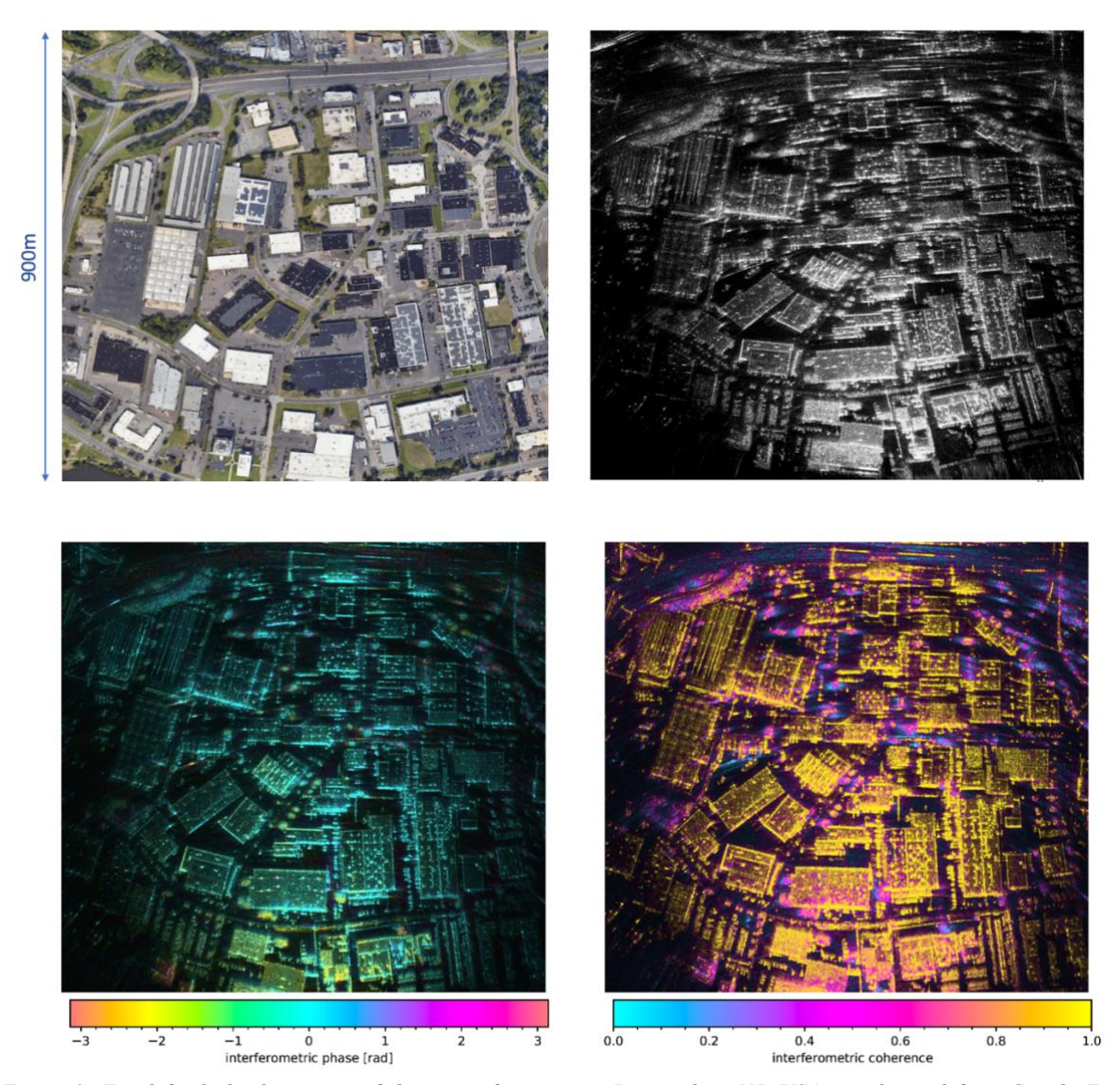


Figure 3: Top left: Orthophoto view of the area of interest in Pennsauken, NJ, USA, as obtained from Google Earth. Single-look intensity SAR image (top right), interferometric phase (bottom left) and interferometric coherence (bottom right) as obtained from quad-copter UAV-borne repeat-pass SAR imagery with the Gamma L-Band SAR system flown on a Freefly Alta X drone (see also Figure 1) with a Honeywell HGuide n500 navigation system built into the radar electronics assembly. The SAR image has a nominal range resolution of 0.75m (200MHz radar signal bandwidth), and a synthetic aperture of approx. 200m, which leads to spatial resolution in azimuth (parallel to flight direction) of approx. 0.2-0.5m (at 1km). A nominal zero-baseline repeat-track interferometric acquisition was taken at a height of approx. 120m above ground in western direction about 100m South of the image shown.



Multi-copter UAV-borne polarimetric SAR imaging at S-band

Another multi-copter UAV-borne SAR image is shown in Figure 4. The data was acquired with the 400MHz-bandwidth Gamma S-band SAR system operated from a Harris HX8 drone in fully-polarimetric mode using the alternating transmit mode (TMA), switching between H-pol and V-pol transmission and simultaneously receiving data with two of the four receiver channels. Detailed features are recognizable due to the high spatial resolution (<40cm) including man-made objects (houses, roof structure, fences), trees and shadows of trees, surface structure in agricultural fields, and power lines. See also reference [13] for more information.

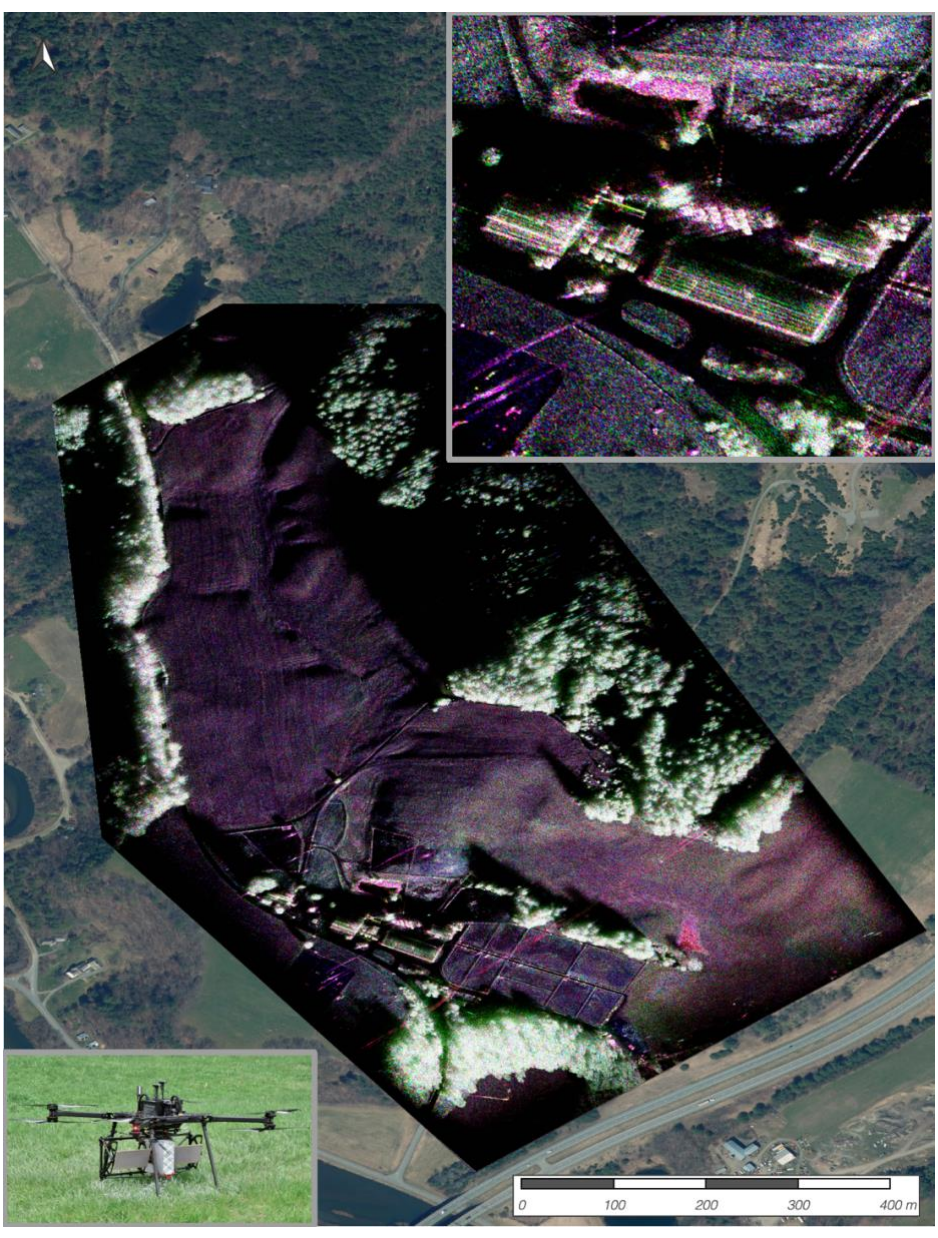


Figure 4: High-resolution (<40cm) fully-polarimetric SAR image at S-Band acquired with the Gamma S-Band SAR system mounted on a Harris HX8 octocopter drone (lower left). The drone was flown 120m above ground in west-southwestern direction along the highway with the radar antennas looking to the right. The false-color RGB image contains the Pauli decomposition with the following components: red: dihedral (even-bounce) scattering, (S_{HH} - S_{VV})/sqrt(2), green: volume scattering: sqrt(2) S_{HV}, blue: surface (single-bounce) and odd-bounce scattering: (S_{HH} + S_{VV})/sqrt(2). A zoomed view of the area around the farm house is shown at the top right. See also Frey et al. 2025 [13] for drone-based repeat-pass InSAR results at S-band and further examples. The drone SAR campaign was carried out in collaboration with the Cold Regions Research and Engineering Laboratory (CRREL), US Army Corps of Engineers. Orthophoto: Vermont Center for Geographic Information, Orthophoto Color Imagery, Statewide (0.3m) 2024. Vermont Open Geodata Portal. https://geodata.vermont.gov.



Demonstration of UAV-borne L-band repeat-pass InSAR

As another example, linear repeat-pass sensor trajectories within a valley can be flown to assess the line-of-sight displacement of a valley slope, irrespective of the direct accessibility of the terrain on the ground. In 2019, a repeat-pass interferometric campaign has been conducted with the first version of the GAMMA L-band SAR mounted on the VTOL UAV Scout B1-100 by Aeroscout GmbH⁶ demonstrating SAR imaging and short-term interferometric phase and coherence of excellent quality (see Figure 5).



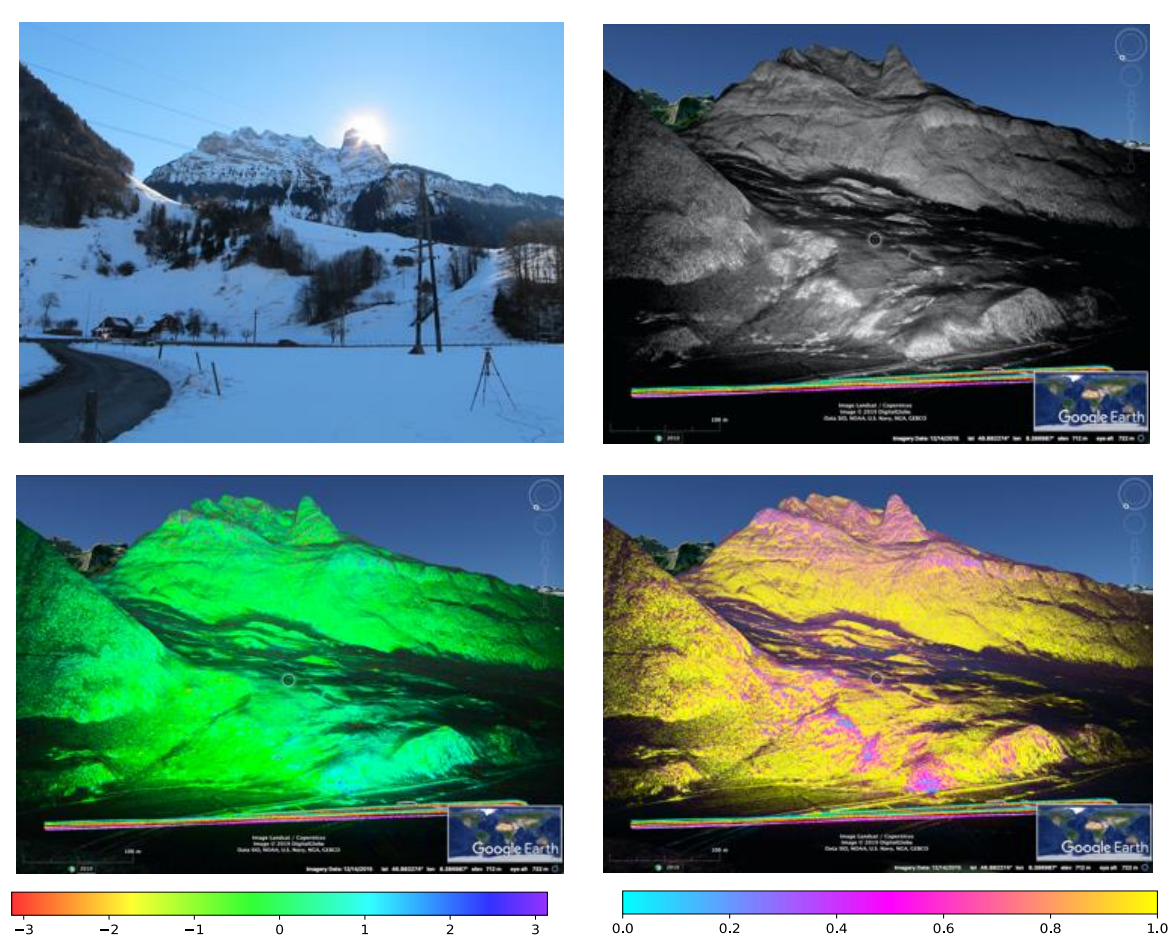


Figure 5: Top right: GAMMA L-band SAR on Aero scout's VTOL UAV Scout B1-100, equipped with a Honeywell HGuide n580 GNSS/INS navigation system, at the test site Wolfenschiessen, Switzerland. Mid-left: Area of interest on the campaign day. On the lower right, the local GNSS reference station is situated to obtain a highly precise post-processed kinematic GNSS solution of the UAV position. Mid-right: Google Earth view of UAV-borne SAR backscatter intensity image with UAV flight trajectories in the foreground. Bottom row: Google Earth view of UAV-borne L-band differential interferometric phase (left) and coherence (right) for nominally zero spatial baseline and a temporal baseline of 3 minutes. The flight tube of these two repeat-tracks is within 1m radius. Except for forested areas in the near range and areas with severe foreshortening a very high coherence is obtained, and the interferometric phase is also stable.

⁶ Note: the demonstration campaign has been conducted in winter with snow cover in the area of interest. This is not recommended for repeat-pass interferometric campaigns with regard to temporal decorrelation. The purpose of this demonstration campaign was to show the technical repeat-pass InSAR capability of the UAV-borne GAMMA L-band SAR data acquisition and TDBP SAR processing system.



Demonstration of car-borne L-band repeat-pass InSAR

Here, we present a repeat-pass interferometric phase measurements of the LOS phase induced by the flow velocity of an alpine glacier obtained in Fall 2018 with the GAMMA L-band SAR. In this demonstration case, the GAMMA L-band SAR system was operated in a car-borne mode: several repeat-pass SAR acquisitions of an alpine glacier are taken from a car driven along a slightly curved section of a mountain road in central Switzerland. The acquired SAR data is focused directly to map coordinates using a digital elevation model with TDBP focusing. Differential interferograms can then be calculated in map coordinates from the geocoded SLC data. Repeat-pass interferometry using GAMMA L-band SAR on an agile mobile mapping platform was successfully demonstrated with these examples (Figures 6-8).



Figure 6: Left/center-left: car-borne setup of the L-band SAR system with one transmit and three receive antennas. Repeated SAR data acquisitions of the Stein Glacier were made while driving on a slightly curved section of mountain road. Center-right/right: Google Earth view of the Stein Glacier test site (CH). Geocoded intensity image (right) overlaid to Google Earth view as obtained from a car-borne L-band SAR acquisition.

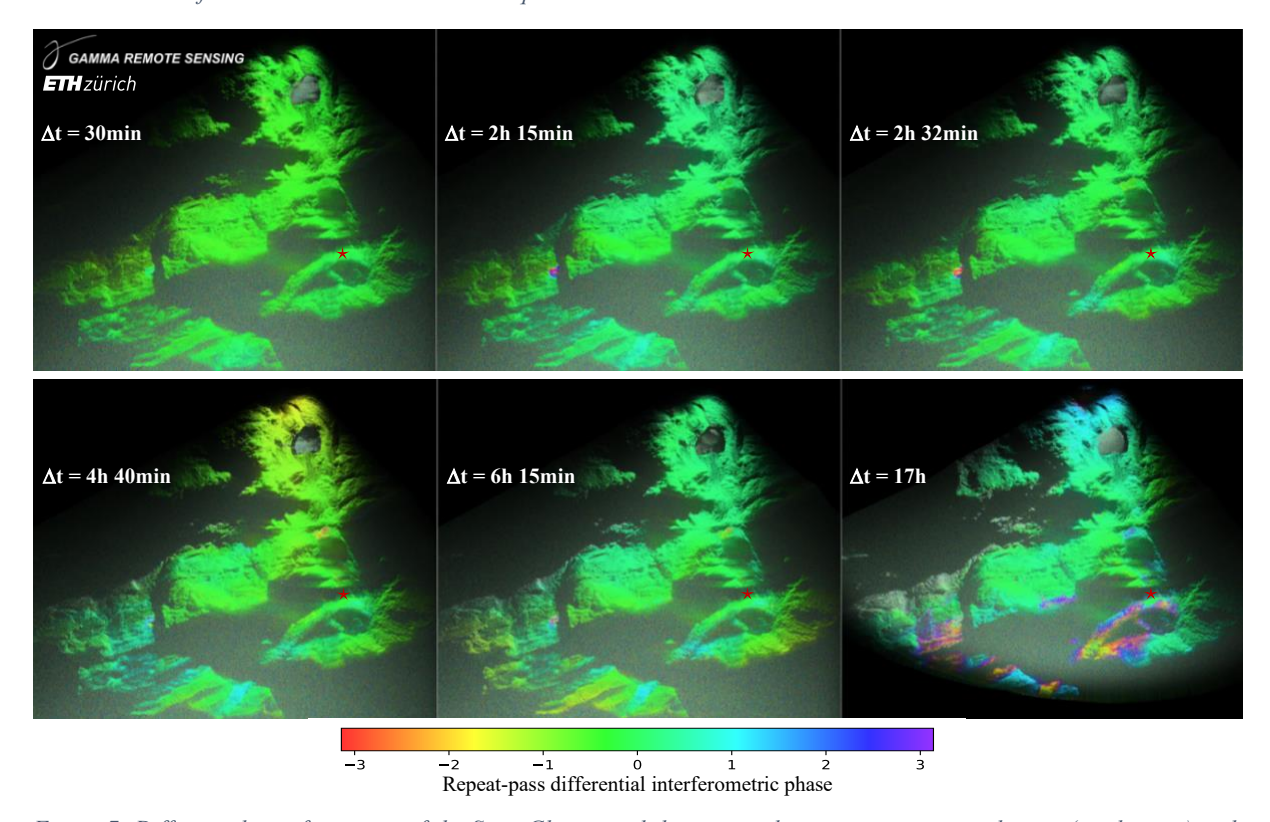


Figure 7: Differential interferograms of the Stein Glacier and the surrounding area in map coordinates (north = up) with temporal baselines of 30 min (upper left), 135 min (upper center), and 152 min (upper right), 280 min (lower left), 375 min (lower center), and 1020 min (=17h) (lower right). The 17h interferogram is obtained between two acquisitions with 1ms chirp duration: hence the limited range distance of ca. 4.68 km. All other interferograms shown are based on acquisitions with 2ms chirp duration. With a carrier frequency of 1.325 GHz (wavelength of 22.6 cm) an interferometric phase value of 2π translates to a line-of-sight displacement of 11.3 cm.



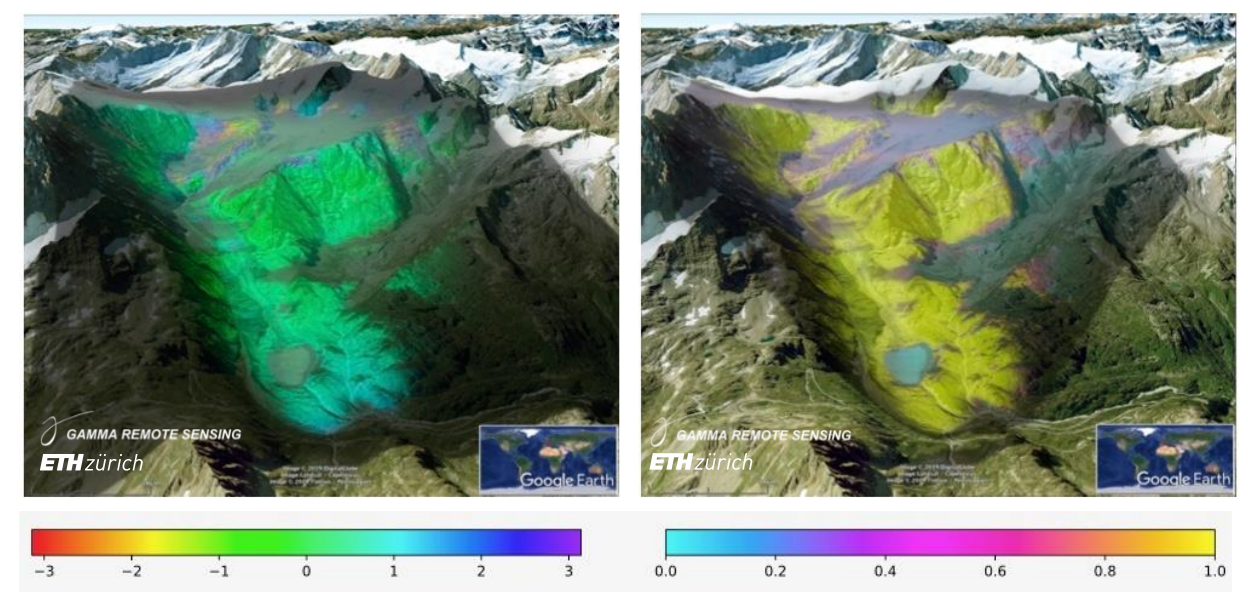


Figure 8:Differential interferogram (left) and coherence magnitude (right)—each blended with a multi-look intensity image—with a temporal baseline of 1020 min (17h) of the Stein Glacier and surrounding area in a 3-D view. The view position of the visualization is above the road section where the car-borne acquisition took place, otherwise looking roughly in the main line-of-sight direction of the radar.

A summary of these results is also available in the citable reference [8].

Mobile mapping of surface displacements of a fast-moving landslide using car-borne L-band repeat-pass InSAR

In this application case mobile mapping of surface displacements of a fast-moving landslide and the surrounding area, in Brinzauls, Switzerland, is shown. This is a typical use case in which the car-borne system setup can be employed (Figure 9). Examples of results obtained are shown in Figure 10. More details can be found in reference [10]. This example was produced using a previous version of the Gamma L-band SAR system with very similar characteristics except the somewhat larger dimensions, the heavier weight, and a different enclosure of the radar electronics assembly.



Figure 9:Car-borne Gamma L-band SAR setup with Honeywell HGuide n580 GNSS/INS system at the Brinzauls landslide.



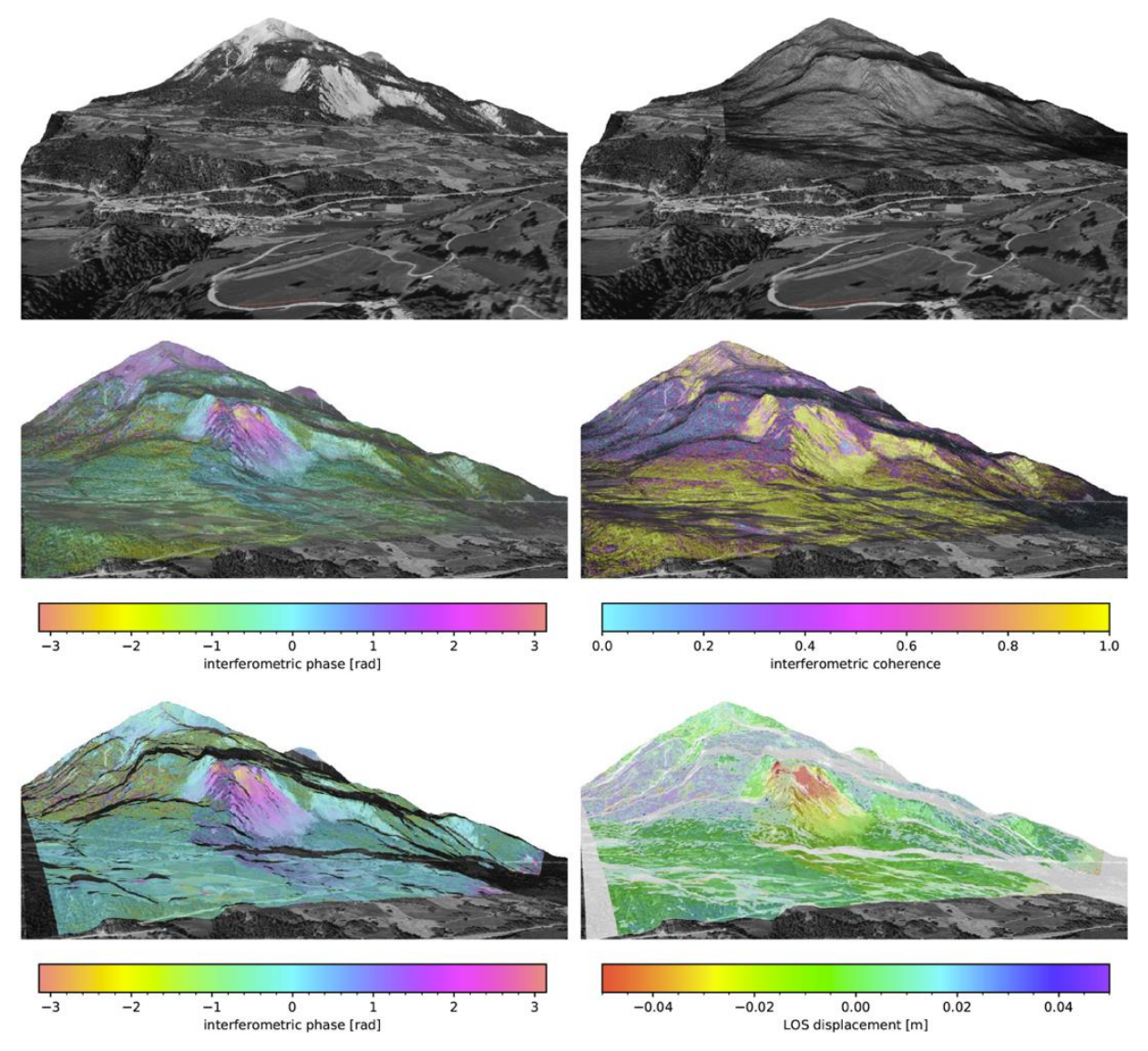


Figure 10:Upper left: 3-D rendering of the test site with the landslide in Brinzauls, Switzerland. Orthophoto and digital elevation model ©swisstopo. The sensor trajectory of the car-borne reference L-band SAR data acquisition is shown as red curved line. Upper right: Overlay of reference SAR image (geoslc), focused directly to the 3-D topography represented by the DEM in map coordinates, and the orthophoto-rendered scene. Middle row: car-borne SAR 4-day unwrapped differential interferogram (left, rewrapped color scale) and coherence (right)—each blended with a multi-look intensity image. Lower left: tropospheric-phase corrected detrended 4-day unwrapped differential interferogram with shadow mask and view mask applied (rewrapped color scale). Lower right: line-of-sight (LOS) displacement observed over 4 days (between 2020-01-20, 14:21and 2020-01-24, 11:25).



In August 2024, we also performed car-borne S-band repeat-pass interferometry at the Brinzauls landslide. In Figure 11, short-term (5 min) and 40-hour interferometric phase and coherence maps are shown indicating the high-resolution mapping capability of the 400MHz bandwidth Gamma S-band SAR system and the excellent repeat-pass interferometric performance of the system for landslide deformation mapping.

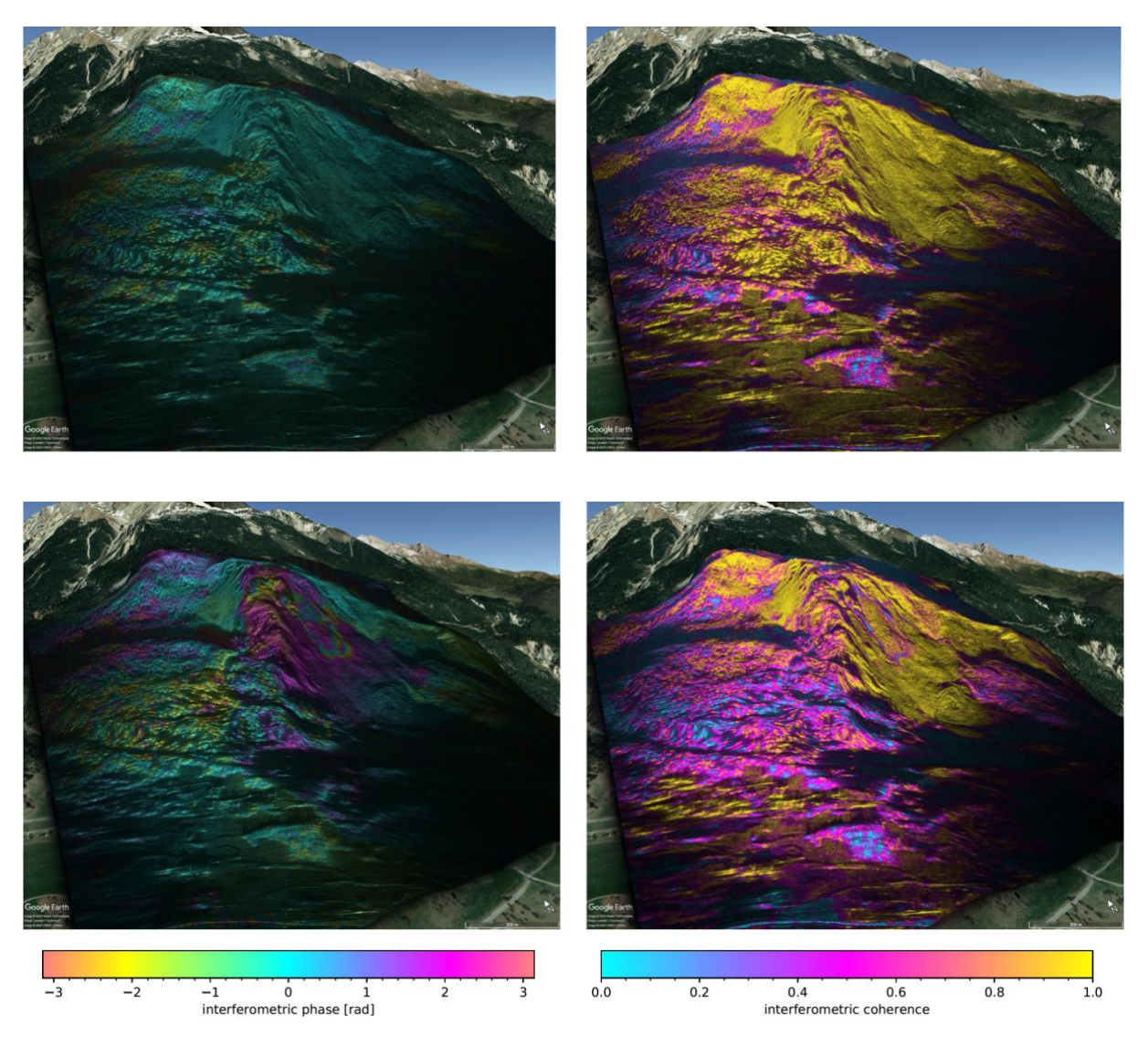


Figure 11: Car-borne repeat-pass SAR interferometry with the Gamma S-Band SAR (400MHz bandwidth) at the Brinzauls landslide in Switzerland: short-term (5min interval) repeat-pass interferometric phase (top left) and coherence map (top right) and 40-hour repeat-pass interferometric phase (bottom left) and coherence map (bottom right).



System Parameter	Gamma L-Band SAR	Gamma S-Band SAR
Operating frequency	1.2-1.4GHz	3.0-3.4GHz
Slant range resolution (3dB)	0.75m @200 MHz BW	0.38 m @400 MHz BW
Azimuth resolution (3dB)	<0.2-0.5m @ full SA	<0.2-0.5m @ full SA
Transmitter output power	programmable, max. 10W	programmable, max. 8W
Number of transmit and receive channels	2 transmit, 4 receive transmit modes: single port (TM1, TM2) or alternating (TMA)	
Radar antenna elevation beam width (3 dB, 1-way)	40 deg	37 deg
Radar antenna azimuth beam width (3 dB, 1-way) *	40 deg or 20 deg	17 deg or 10 deg
Antenna gain	16dBi or 13dBi	18.5dBi or 15.5dBi
Polarization	H and V	
Dimensions of the radar (radar electronics assembly)	100 x 254 x 254 mm	
Dimension including carbon frame	381 x 1243 x 383 mm	
Mass (radar instrument (REA)	4.2kg	
Total mass (radar instrument, carbon frame, 2 radar antennas, 2 GNSS antennas, cables)	6.5 kg	
Power consumption	45 W idle, 90 – 110 W transmit (140 W max).	
DC power input	44 VDC (31 to 54 V)	
Onboard SSD data storage	2 TB, 1.7 TB for radar data	
I/O interfaces	Gigabit Ethernet, USB3, Serial, GPIO	
Environmental	IP 65, Temp.: -35 to +40 C	
Built-in GNSS/INS nav. system	Honeywell n500 INS + NovAtel OEM7720 GNSS	

Table 1:System specifications of the Gamma L-Band SAR and Gamma S-Band SAR systems



References

- Frey, O., Werner, C. L., and Wegmüller, U.: "GPU-based parallelized time-domain back-projection processing for agile SAR platforms," in Proc. IEEE Int. Geosci. Remote Sens. Symp., July 2014, pp. 1132–1135. [Online]. Available: https://ieeexplore.ieee.org/document/6946629
- 2. Frey, O., Magnard, C., Rüegg, M., and Meier, E.: "Focusing of airborne synthetic aperture radar data from highly nonlinear flight tracks," IEEE Trans. Geosci. Remote Sens., vol. 47, no. 6, pp. 1844–1858, June 2009. [Online]. Available: https://ieeexplore.ieee.org/document/4812049
- Frey, O., Meier, E., and Nüesch, D.: "Processing SAR data of rugged terrain by time-domain back-projection," in SPIE Vol. 5980: SAR Image Analysis, Modeling, and Techniques X, 2005. [Online]. Available: https://doi.org/10.1117/12.627647
- 4. Ribalta, A.: "Time-domain reconstruction algorithms for FMCW- SAR," IEEE Geoscience and Remote Sensing Letters, vol. 8, no. 3, pp. 396–400, May 2011.
- 5. Stringham, C. and Long, D. G.: "GPU processing for UAS-based LFM-CW stripmap SAR," Photogrammetric Engineering & Remote Sensing, vol. 80, no. 12, pp. 1107–1115, 2014.
- Frey, O., Werner, C. L., Wegmüller, U., Wiesmann, A., Henke, D., and Magnard, C.: "A car-borne SAR and InSAR experiment," in Proc. IEEE Int. Geosci. Remote Sens. Symp., 2013, pp. 93–96 [Online]. Available: https://ieeexplore.ieee.org/document/6721100
- 7. Frey, O., Werner, C. L., Hajnsek, I., and Coscione, R.: "A car-borne SAR system for interferometric measurements: development status and system enhancements," in Proc. IEEE Int. Geosci. Remote Sens. Symp., 2018, pp. 6508–6511. [Online]. Available: https://ieeexplore.ieee.org/document/8518840
- 8. Frey, O., Werner, C. L., Coscione, R.: "Car-borne and UAV-borne mobile mapping of surface displacements with a compact repeat-pass interferometric SAR system at L-band," Proc. IEEE Int. Geosci. Remote Sens. Symp., July/Aug 2019, pp. 274-277. [Online]. Available: https://doi.org/10.1109/IGARSS.2019.8897827
- 9. Frey, O., and Werner, C. L.: "UAV-borne repeat-pass SAR interferometry and SAR tomography with a compact L-band SAR system," in Proc. Europ. Conf. Synthetic Aperture Radar, EUSAR, Mar. 2021, pp. 181–184. [Online]. Available: https://ieeexplore.ieee.org/document/9553573
- Frey, O., Werner, C. L., Manconi, A., Coscione, R.: "Measurement of surface displacements with a UAV-borne/car-borne L-band DInSAR system: system performance and use cases," in Proc. IEEE Int. Geosci. Remote Sens. Symp., 2021, pp. 628–631. [Online]. Available: https://doi.org/10.1109/IGARSS47720.2021.9553573
- 11. Frey, O., Werner, C., and Caduff, R.: "Car-borne Mobile Mapping of Ground Motion by Means of Repeat-Pass SAR Interferometry: Case Studies and Application Development Based on L-Band and Ku-band SAR Data Acquisitions," in Proc. IEEE Int. Geosci. Remote Sens. Symp., Pasadena: IEEE, Jul. 2023, pp. 1902–1905. [Online]. Available: https://doi.org/10.1109/IGARSS52108.2023.10283211
- Frey, O., Werner, C.L., Caduff, R.: "Simultaneous Car-Borne SAR Imaging at L-Band and Ku-Band for DInSAR-Based Mobile Mapping of Ground Motion in Alpine Terrain," in Proc. of EUSAR 2024, Munich, Germany: VDE, Apr. 2024, pp. 1259–1264. [Online]. Available: https://www.gamma-rs.ch/uploads/media/freyEtAlEUSAR2024CarborneDInSARBrinzaulsKuAndLBand.pdf
- 13. Frey, O.; Werner, C.; Leinss, S.; Batt, T.; Caduff, R.; Dixon, T.; Sadeghi Chorsi, T.; Van Alphen, R.; Schmitt, M.; Eitel, M.; Sica, F.; Deeb, E. J.; LeWinter, A. L.; Filiano, D. L.; Wagner, C. J. & Hoppinen, Z., "Multicopter-UAV- and car-borne repeat-pass SAR interferometry and SAR tomography with the compact Gamma SAR systems: first examples and use cases at S- and L-band," in Proc. IEEE Int. Geosci. Remote Sens. Symp., Brisbane, Australia: IEEE, Aug. 2025, pp. 1374–1377. [Online]. Available: https://www.gamma-rs.ch/uploads/media/freyEtAlIGARSS2025GammaSARCarAndUAVBorneLBandandSBand.pdf
- 14. Strozzi, T., Caduff, R., Bernhard, P., Frey, O., Wegmüller, U., Manconi, A., Agliardi, F., de Pedrini, A. & Ambrosi, C., "Integration of multi-sensor L-band DInSAR surface motion products for landslide monitoring," in Proc. IEEE Int. Geosci. Remote Sens. Symp., Brisbane, Australia, Aug. 2025, pp. 9095–9098. [Online]. Available: https://www.gamma-rs.ch/uploads/media/strozziEtAlIGARSS2025MODULATE.pdf



Sales information

The Gamma SAR Systems are commercial products available for purchase. To obtain a price list or a specific offer please contact: instruments@gamma-rs.ch.

Gamma Remote Sensing also offers customization of the Gamma SAR systems according to specific needs as well as support and consulting for customers who would like to integrate the Gamma SAR System onto their platform of choice (car, UAV, airplane).

In addition, Gamma Remote Sensing offers services – e.g. monitoring of ground motion using car-borne DInSAR with the Gamma L-band SAR system, which can also be complemented with spaceborne DInSAR / persistent scatterer interferometry analyses and stationary terrestrial radar interferometry using the Ku-band GPRI – and customized application development.

Further information is available at http://www.gamma-rs.ch.

Further references

Several papers are available that document a specific element or functionality of the GAMMA SAR Systems and the TDBP SAR processing approach. A list of these documents with links to download the individual pdf files is also available at:

https://www.gamma-rs.ch/publications-gamma-sar-systems